

EFFECTS OF ULTRAVIOLET BACKGROUND AND LOCAL STELLAR RADIATION ON THE H I COLUMN DENSITY DISTRIBUTION

KENTARO NAGAMINE^{1,3}, JUN-HWAN CHOI^{1,4}, HIDENOBU YAJIMA²

Draft version June 8, 2018

ABSTRACT

We study the impact of ultraviolet background (UVB) radiation field and the local stellar radiation on the H I column density distribution $f(N_{\text{HI}})$ of damped Ly α systems (DLAs) and sub-DLAs at $z = 3$ using cosmological smoothed particle hydrodynamics simulations. We find that, in the previous simulations with an optically thin approximation, the UVB was sinking into the H I cloud too deeply, and therefore we underestimated the $f(N_{\text{HI}})$ at $19 < \log N_{\text{HI}} < 21.2$ compared to the observations. If the UVB is shut off in the high-density regions with $n_{\text{gas}} > 6 \times 10^{-3} \text{ cm}^{-3}$, then we reproduce the observed $f(N_{\text{HI}})$ at $z = 3$ very well. We also investigate the effect of local stellar radiation by post-processing our simulation with a radiative transfer code, and find that the local stellar radiation does not change the $f(N_{\text{HI}})$ very much. Our results show that the shape of $f(N_{\text{HI}})$ is determined primarily by the UVB with a much weaker effect by the local stellar radiation and that the optically thin approximation often used in cosmological simulation is inadequate to properly treat the ionization structure of neutral gas in and out of DLAs. Our result also indicates that the DLA gas is closely related to the transition region from optically-thick neutral gas to optically-thin ionized gas within dark matter halos.

Subject headings: cosmology: theory — galaxies: evolution — galaxies: formation — galaxies: high-redshift — quasars: absorption lines — methods: numerical

1. INTRODUCTION

The H I column density distribution function $f(N_{\text{HI}})$ is one of the most basic statistics of quasar absorption systems, similarly to the luminosity function of galaxies. The accuracy of observational data on $f(N_{\text{HI}})$ has dramatically improved over the past several years, thanks to the large samples of damped Ly α systems (DLAs) and sub-DLAs discovered in large data sets of quasar spectra (e.g., Péroux et al. 2003; Prochaska & Herbert-Fort 2004; Péroux et al. 2005; Prochaska et al. 2005, 2008; Noterdaeme et al. 2009). Their results indicate that the observed $f(N_{\text{HI}})$ of DLAs can be fitted well with either a double power-law or a Schechter-type function.

It would be desirable to understand the physical origin of the shape of $f(N_{\text{HI}})$ in a cosmological context of the standard Λ cold dark matter model. The first such attempt was made by Katz et al. (1996b), who used a cosmological smoothed particle hydrodynamics (SPH) simulation with a comoving box-size of $22.22h^{-1} \text{ Mpc}$, 2×64^3 particles, and cosmological parameters $(\Omega_m, \Omega_\Lambda, \Omega_b) = (1.0, 0.0, 0.05)$. They found that their simulation underpredicted $f(N_{\text{HI}})$ compared to the observational data by a factor of few or more, using a uniform ultraviolet background (UVB) $J(\nu) = J_0(\nu_0/\nu)$ at $z = 3$, where ν_0 is the Lyman-limit frequency and

$J_0 = 10^{-22} \text{ erg s}^{-1} \text{ cm}^{-2} \text{ sr}^{-1} \text{ Hz}^{-1}$. The UVB is usually treated with an optically thin limit regardless of gas density in cosmological hydrodynamic simulations owing to the computational limit. This simplified approximation may artificially increase the ionization fraction of gas, and gives rise to the discrepancy in $f(N_{\text{HI}})$.

Nagamine et al. (2004, 2007) updated the work of Katz et al. (1996b) using cosmological SPH simulations with a comoving box size of $10h^{-1} \text{ Mpc}$, 2×324^3 particles, and $(\Omega_m, \Omega_\Lambda, \Omega_b) = (0.3, 0.7, 0.044)$. Interestingly, they also found a similar underprediction of $f(N_{\text{HI}})$ compared to the observations, despite significantly higher resolution than that of Katz et al. (1996b). Their simulations included a uniform UVB of Haardt & Madau (1996) spectrum, modified by Davé et al. (1999) to match the Ly α forest observations.

We have attempted to resolve this discrepancy by modifying the models of star formation (SF) and supernova feedback; e.g., changing the SF threshold density, SF time-scale, feedback strengths, or adding metal-line cooling (Choi & Nagamine 2009b,a). However, none of these changes in the physical models resolved the discrepancy in $f(N_{\text{HI}})$ fundamentally.

In this Letter, we show that the effect of UVB is the key in determining the shape of $f(N_{\text{HI}})$ at $\log N_{\text{HI}} \lesssim 21.6$. In addition, we consider the effect of local stellar radiation on $f(N_{\text{HI}})$ by performing a radiative transfer (RT) calculation. Our paper is organized as follows. In Section 2, we briefly describe the setup of our simulations, and present the results in Section 3. We then discuss the comparison with other recent works, and conclude in Section 4.

2. SIMULATIONS

We use the updated version of the tree-particle-mesh SPH code GADGET-3 (originally described in Springel

¹ Department of Physics & Astronomy, University of Nevada Las Vegas, 4505 Maryland Pkwy, Box 454002, Las Vegas, NV 89154-4002 USA; kn@physics.unlv.edu

² Department of Astronomy and Astrophysics, Pennsylvania State University, 525 Davey Lab, University Park, PA 16802, USA

³ Visiting Researcher, Institute for the Physics and Mathematics of the Universe, University of Tokyo, 5-1-5 Kashiwanoha, Kashiwa, 277-8568, Japan

⁴ Current address: Department of Physics and Astronomy, University of Kentucky, Lexington, KY 40506-0055, USA

2005). Our conventional code includes radiative cooling by H, He, and metals (Choi & Nagamine 2009a), heating by a uniform UVB of a modified Haardt & Madau (1996) spectrum (Katz et al. 1996a; Davé et al. 1999), SF, supernova feedback, a phenomenological model for galactic winds, and a sub-resolution model of multiphase interstellar medium (ISM; Springel & Hernquist 2003). In this multiphase ISM model, high-density ISM is pictured to be a two-phase fluid consisting of cold clouds in pressure equilibrium with a hot ambient phase. Cold clouds grow by radiative cooling out of the hot medium, and this material forms the reservoir of baryons available for SF. We use the “Pressure SF” model described by Choi & Nagamine (2010) (which is based on the work by Schaye & Dalla Vecchia (2008)), but we have checked that the details of the SF model do not change the main conclusions of this paper.

For all the simulations used in this paper, we employ a box size of comoving $10 h^{-1}$ Mpc and a total particle number of 2×144^3 for gas and dark matter. The initial gas particle mass is $m_{\text{gas}} = 4.1 \times 10^6 h^{-1} M_{\odot}$, and the dark matter particle mass is $m_{\text{dm}} = 2.0 \times 10^7 h^{-1} M_{\odot}$. The comoving gravitational softening length is $2.78 h^{-1}$ kpc, so the physical resolution of our simulation is $\sim 0.7 h^{-1}$ kpc at $z = 3$. Nagamine et al. (2004) showed that increasing the particle number from 2×144^3 to 2×324^3 did not change the shape of $f(N_{\text{HI}})$ very much, therefore our results would not be strongly affected by the resolution effect. (But see further discussion in Section 4.) The comoving box size of $10 h^{-1}$ Mpc is somewhat small, however, the number of missed very massive haloes are relatively small, and the impact on $f(N_{\text{HI}})$ is expected to be small. In fact Nagamine et al. (2004) showed that $f(N_{\text{HI}})$ did not change very much with increasing box size, except that the lower N_{HI} end of $f(N_{\text{HI}})$ decreased due to lower resolution. In this work, we have not corrected our results for the box size effect. The adopted cosmological parameters of all simulations are consistent with the latest WMAP result (Komatsu et al. 2009, 2010): $(\Omega_m, \Omega_{\Lambda}, \Omega_b, \sigma_8, h, n_s) = (0.26, 0.74, 0.044, 0.80, 0.72, 0.96)$, where $h = H_0/(100 \text{ km s}^{-1} \text{ Mpc}^{-1})$.

With this setup, we run four simulations with different models of UVB: “Fiducial”, “No-UV”, “Half-UV”, and “OTUV” (Optically Thick UV) runs. In the Fiducial run, the gas is heated and ionized by the uniform UVB under the optically thin approximation. In the No-UV run, the UVB strength is set to zero. In the Half-UV run, the normalization of UVB is reduced by half. In the OTUV run, we assume that the uniform UVB cannot penetrate into the high-density gas with $n_{\text{gas}} > n_{\text{th}}^{\text{UV}}$, but otherwise it is the same as the Fiducial run at $n_{\text{gas}} \leq n_{\text{th}}^{\text{UV}}$.

We adopt the threshold density $n_{\text{th}}^{\text{UV}} = 0.01 n_{\text{th}}^{\text{SF}} = 6 \times 10^{-3} \text{ cm}^{-3}$, where $n_{\text{th}}^{\text{SF}}$ is the SF threshold density above which the stars are allowed to form. In our simulations, the gas with $n_{\text{gas}} > n_{\text{th}}^{\text{SF}}$ is mostly neutral owing to the multiphase ISM model. We originally arrived at the above value of $n_{\text{th}}^{\text{UV}}$ by successively lowering its value from $n_{\text{th}}^{\text{SF}}$ and checking the agreement with the observed $f(N_{\text{HI}})$, but will provide further justifications below.

There is evidence that the above value of $n_{\text{th}}^{\text{UV}}$ is phys-

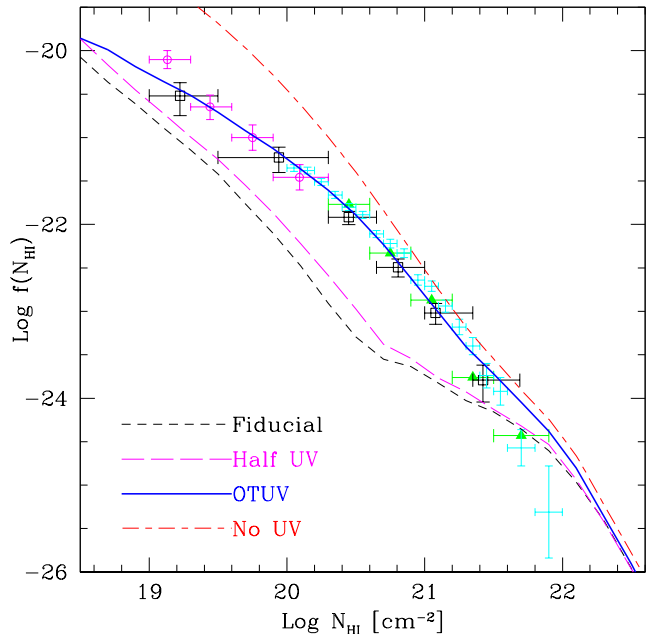


FIG. 1.— H I column density distribution functions at $z = 3$ for the four runs with different treatment of UVB. The observational data points are from Péroux et al. (2005, black open squares), O’Meara et al. (2007, magenta open circles), Prochaska & Wolfe (2009, green triangles), and Noterdaeme et al. (2009, cyan bars).

ically appropriate. Tajiri & Umemura (1998) found that the hydrogen cloud becomes fully self-shielded above a critical density of $1.4 \times 10^{-2} \text{ cm}^{-3}$ through RT calculations for a spherical top-hat sphere, and that the critical density has a mild dependence on the cloud mass and the UVB intensity. Kollmeier et al. (2010) performed a three-dimensional UVB RT calculation with an isothermal sphere, and showed that the above value of $n_{\text{th}}^{\text{UV}}$ approximately corresponds to the transition density from H II to H I. Faucher-Giguere et al. (2010) postprocessed cosmological SPH simulations with a ray tracing code and found that turning off UVB at $n_{\text{gas}} > 0.01 \text{ cm}^{-3}$ produces a favorable result. Furthermore, we also confirmed that the above $n_{\text{th}}^{\text{UV}}$ is appropriate by postprocessing our simulations with a RT code, which we will report in detail in a separate paper (H. Yajima et al., 2011, in preparation). For these reasons, we consider that the correct value of $n_{\text{th}}^{\text{UV}}$ is in the range of 10^{-2} to 10^{-3} cm^{-3} , depending on the cloud mass and UVB intensity.

3. RESULTS

3.1. Effect of UVB on $f(N_{\text{HI}})$

Figure 1 shows the $f(N_{\text{HI}})$ in the four runs with different UVB treatment, which was calculated by the same method described in Nagamine et al. (2004). In short, we set up a uniform grid around each dark matter halo, and project the gas density field onto a face of the grid to compute N_{HI} . Figure 1 clearly shows that the Fiducial run underpredicts the $f(N_{\text{HI}})$, particularly at $\log N_{\text{HI}} < 21.2$. The Half-UV run is somewhat higher than the Fiducial run, but still not enough to account for the observed number of columns at $19.5 < \log N_{\text{HI}} < 21$. On the other hand, the No-UV run completely overpredicts

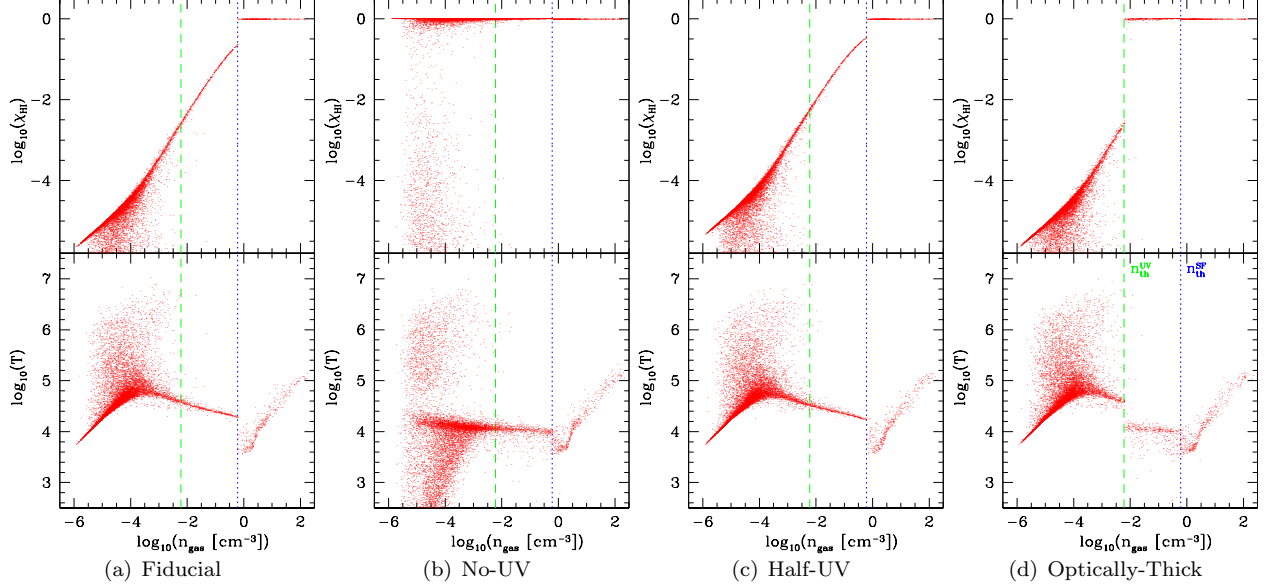


FIG. 2.— Neutral hydrogen fraction (n_{gas} vs. χ_{HI} ; top panels) and phase space distribution (n_{gas} vs. T ; bottom panels) of the cosmic gas at $z = 3$ for the four runs. The neutral fraction is defined as $\chi_{\text{HI}} = n_{\text{HI}}/(n_{\text{HI}} + n_{\text{HII}})$. For plotting purpose, we plot only randomly selected 1% of the total gas particles in the simulation. The two densities, $n_{\text{th}}^{\text{UV}}$ and $n_{\text{th}}^{\text{SF}}$, are indicated by the vertical green dashed line and blue dotted lines, respectively.

the observed $f(N_{\text{HI}})$ at all column densities. The sudden decrease in $f(N_{\text{HI}})$ from the No-UV run to the Half-UV run shows that even a weak UVB can ionize the gas and the simulation cannot account for the observed number of columns. The OTUV run agrees very well with the observed data at $19.2 < \log N_{\text{HI}} < 21.2$. The comparison of these four runs suggests that the UVB affects the shape of $f(N_{\text{HI}})$ significantly, and that applying the optically thin approximation at all densities is too simplistic to reproduce the observed $f(N_{\text{HI}})$ properly. Our simulations overpredict $f(N_{\text{HI}})$ at $\log N_{\text{HI}} > 10^{22} \text{ cm}^{-2}$. But this could be because our simulations do not take into account the conversion of H I into H₂, and the conclusion of this paper does not depend on this issue.

To obtain a better physical intuition on the effect of UVB, we plot the hydrogen neutral fraction (χ_{HI}) and temperature against gas density for the four runs in Figure 2. The difference of $f(N_{\text{HI}})$ between the Fiducial and the OTUV run must be due to the different neutral fraction of gas at $n_{\text{th}}^{\text{UV}} < n_{\text{gas}} < n_{\text{th}}^{\text{SF}}$ in the two runs. The Fiducial run predicts a high degree of ionization at $n_{\text{gas}} < n_{\text{th}}^{\text{SF}}$ ($\approx 0.6 \text{ cm}^{-3}$). For example, the gas with $n_{\text{gas}} \sim 0.1 \text{ cm}^{-3}$ at $z = 3$ has $\chi_{\text{HI}} \sim 0.05$ for the Fiducial run. By referencing to $f(N_{\text{HI}})$, the gas with this density should correspond to the DLAs with $\log N_{\text{HI}} \sim 20$, and $\chi_{\text{HI}} \sim 0.05$ is too low to match the observed data on $f(N_{\text{HI}})$. The Half-UV run has a higher neutral fraction for the gases with $n_{\text{gas}} < n_{\text{th}}^{\text{SF}}$, but still with $\chi_{\text{HI}} < 0.3$. In contrast, most hydrogen in the No-UV run has $\chi_{\text{HI}} \sim 1.0$, except for the small fraction of hot gas which is ionized by collisional ionization in shocked regions. Eliminating the UVB completely is not a realistic assumption, and the No-UV run clearly overpredicts $f(N_{\text{HI}})$ as expected. Lastly, in the OTUV run, the gas with $n_{\text{gas}} > n_{\text{th}}^{\text{UV}}$ has $\chi_{\text{HI}} \sim 1.0$, which allows it to match the observed $f(N_{\text{HI}})$. Figures 1 and 2 clearly show that the optically thin approximation ionizes the gas with $n_{\text{th}}^{\text{UV}} < n_{\text{gas}} < n_{\text{th}}^{\text{SF}}$

too much. In order to properly reproduce the observed $f(N_{\text{HI}})$ with our simulations, the gas should be mostly neutral at $n_{\text{gas}} > n_{\text{th}}^{\text{UV}}$.

The effects of UVB can also be seen in the $\rho - T$ phase diagrams in the bottom panels of Figure 2. The comparison of the Fiducial and No-UV runs shows the well-known photoionization effect on the diffuse IGM at low densities of $n_{\text{gas}} < 10^{-2} \text{ cm}^{-3}$. Compared to the Fiducial run, the gas with $n_{\text{th}}^{\text{UV}} < n_{\text{gas}} < n_{\text{th}}^{\text{SF}}$ in the OTUV run is almost fully neutral with a lower temperature of $T \sim 10^4 \text{ K}$. We will show in a separate paper (H. Yajima et al., 2011, in preparation) that a full RT calculation supports the results shown in Figure 2(d).

3.2. Effects of Radiative Transfer on $f(N_{\text{HI}})$

The OTUV run is remarkably successful in reproducing the observed $f(N_{\text{HI}})$ at $19 < \log N_{\text{HI}} < 21.5$, but so far we have neglected the radiative effects of the stellar radiation from local stellar sources, which could heat and ionize the high-density gas in the star-forming regions.

In order to consider the effects of local stellar radiation, we postprocess our simulation with the Authentic Radiation Transfer (ART) code (Nakamoto et al. 2001; Yajima et al. 2009), which uses the ray-tracing technique. We have performed the RT calculation in a similar fashion to the one we did in Yajima et al. (2010), taking the RT grid cell size equal to the gravitational softening length. This way the resolution of the RT calculation is fixed for all halos. Figure 3 compares the results from the OTUV run with and without the RT calculation. The transferred stellar spectra are computed by using the PÉGASE v2.0 (Fioc & Rocca-Volmerange 1997) based on the mass, formation time, and age of the star particles generated in the simulation. We find that the local stellar radiation does not have a significant impact on the shape of $f(N_{\text{HI}})$, as shown by the red long-dashed line in Figure 3, which is almost overlapping with the original OTUV run without RT. This is because the stellar

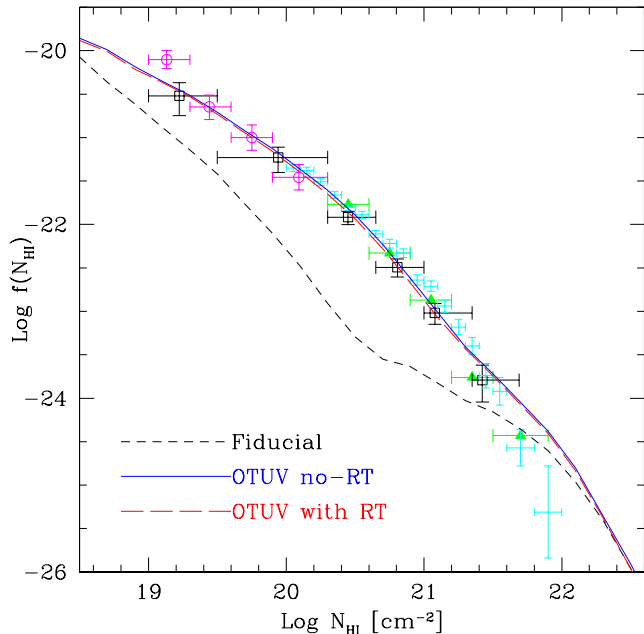


FIG. 3.— Effect of local stellar radiation on $f(N_{\text{HI}})$ at $z = 3$. The observational data points are the same as in Figure 1. The two lines for the OTUV with and without RT (red dashed and blue solid lines, respectively) are almost overlapping with each other.

radiation can only increase the ionization fraction of gas near the ionization boundary where it makes a transition from neutral to highly ionized, and the high density neutral gas remains largely intact. We will report more details of the RT calculation results in a separate publication (H. Yajima et al. 2011, in preparation).

4. DISCUSSIONS AND CONCLUSIONS

Using cosmological SPH simulations, we examined the effects of UVB on $f(N_{\text{HI}})$, and clarified the reason why earlier simulations have underestimated this quantity compared to the observations. We find that the radiation sinks into the halo gas too deeply under the optically thin approximation of UVB, and the gas with $19 < \log N_{\text{HI}} < 21.5$ is overly ionized. If we turn off the UVB above a physical density of $n_{\text{th}}^{\text{UV}} = 6 \times 10^{-3} \text{ cm}^{-3}$, then we reproduce the observed $f(N_{\text{HI}})$ at $z = 3$ very well. The exact value of $n_{\text{th}}^{\text{UV}}$ would depend on the details of the spectral shape and the intensity of UVB, and the size of gas cloud (Tajiri & Umemura 1998). Based on the comparison to other works, we consider that a value of $n_{\text{th}}^{\text{UV}} \sim 10^{-2} - 10^{-3} \text{ cm}^{-3}$ would be appropriate for current cosmological simulations. Our results clearly show that the optically thin approximation was responsible for the failure in matching the observed $f(N_{\text{HI}})$ in earlier simulations.

Recently, problems in the optically thin approximation have been pointed out in the context of the He II reionization effect on the thermal history of IGM (McQuinn et al. 2009; Faucher-Giguère et al. 2009) and Ly- α emission (Yang et al. 2006; Faucher-Giguère et al. 2010). Our present work is another example of inadequacy of optically thin approximation of UVB for modeling the ionization of gas near DLAs. The RT effects, as well as the exact shape of UVB, have significant impact on the details of galaxy formation history including DLAs (e.g., Tajiri & Umemura 1998; Zheng & Miralda-Escudé 2002; Hambrick et al. 2009; Kollmeier et al. 2010; Faucher-Giguère et al. 2010).

Although cosmological RT simulations are beginning to be performed, it is still difficult to do a self-consistent ray-tracing RT calculation concurrently with the hydrodynamics due to limited computational speed. Under this circumstance, it would still help to have a physically plausible working model of self-shielding for cosmological simulations. Our result provides a useful proxy for the threshold density ($n_{\text{th}}^{\text{UV}}$) above which the self-shielding effect kicks in.

We also examined the effects of local stellar radiation by postprocessing the simulation with a ray-tracing code. The effect is not as strong as the UVB, and it only slightly decreases $f(N_{\text{HI}})$. We will report the further details of this ray-tracing work and its effect on DLA cross section in a separate publication (H. Yajima et al. 2011, in preparation).

To put it in another way, our results suggest that the shape of $f(N_{\text{HI}})$ and the ionization structure of sub-DLAs and DLAs would be great probes of UVB at high redshift, and that the DLA gas is closely related to the transition region from optically-thin ionized gas to optically-thick neutral gas within dark matter halos. Further comparisons on the physical properties of DLAs, sub-DLAs, and Lyman limit systems between simulations and observations would give us useful insight on the nature of UVB.

In Section 2 we argued that our results are not strongly affected by the numerical resolution of our current simulations, based on the results of Nagamine et al. (2004). However the simulations of Nagamine et al. (2004) did not include the self-shielding treatment of the OTUV run, so to really test the resolution effect, we would have to run a new OTUV simulation with 2×324^3 particles, which we plan to perform in the near future and address the resolution effects more directly.

ACKNOWLEDGMENTS

This work is supported in part by the NSF Grant AST-0807491, National Aeronautics and Space Administration under Grant/Cooperative Agreement No. NNX08AE57A issued by the Nevada NASA EPSCoR program, and the President's Infrastructure Award from UNLV. KN is grateful for the hospitality of the IPMU at University of Tokyo, where part of this work was performed.

REFERENCES

- Choi, J. & Nagamine, K. 2009a, MNRAS, 393, 1595
- . 2009b, MNRAS, 395, 1776
- . 2010, MNRAS, 407, 1464
- Davé, R., Hernquist, L., Katz, N., & Weinberg, D. H. 1999, ApJ, 511, 521
- Faucher-Giguère, C., Keres, D., Dijkstra, M., Hernquist, L., & Zaldarriaga, M. 2010, arXiv e-prints (arXiv:1005.3041)

- Faucher-Giguère, C., Lidz, A., Zaldarriaga, M., & Hernquist, L. 2009, *ApJ*, 703, 1416
- Fioc, M. & Rocca-Volmerange, B. 1997, *A&A*, 326, 950
- Haardt, F. & Madau, P. 1996, *ApJ*, 461, 20
- Hambrick, D. C., Ostriker, J. P., Naab, T., & Johansson, P. H. 2009, *ApJ*, 705, 1566
- Katz, N., Weinberg, D. H., & Hernquist, L. 1996a, *ApJS*, 105, 19
- Katz, N., Weinberg, D. H., Hernquist, L., & Miralda-Escudé, J. 1996b, *ApJ*, 457, L57
- Kollmeier, J. A., Zheng, Z., Davé, R., Gould, A., Katz, N., Miralda-Escudé, J., & Weinberg, D. H. 2010, *ApJ*, 708, 1048
- Komatsu, E., et al. 2009, *ApJS*, 180, 330
- Komatsu, E., et al. 2010, arXiv e-prints (arXiv:1001.4538)
- McQuinn, M., Lidz, A., Zaldarriaga, M., Hernquist, L., Hopkins, P. F., Dutta, S., & Faucher-Giguère, C. 2009, *ApJ*, 694, 842
- Nagamine, K., Springel, V., & Hernquist, L. 2004, *MNRAS*, 348, 421
- Nagamine, K., Wolfe, A. M., Hernquist, L., & Springel, V. 2007, *ApJ*, 660, 945
- Nakamoto, T., Umemura, M., & Susa, H. 2001, *MNRAS*, 321, 593
- Noterdaeme, P., Petitjean, P., Ledoux, C., & Srianand, R. 2009, *A&A*, 505, 1087
- O’Meara, J. M., Prochaska, J. X., Burles, S., Prochter, G., Bernstein, R. A., & Burgess, K. M. 2007, *ApJ*, 656, 666
- Péroux, C., Dessauges-Zavadsky, M., D’Odorico, S., Sun Kim, T., & McMahon, R. G. 2005, *MNRAS*, 363, 479
- Péroux, C., McMahon, R. G., Storrie-Lombardi, L. J., & Irwin, M. J. 2003, *MNRAS*, 346, 1103
- Prochaska, J. X., Hennawi, J. F., & Herbert-Fort, S. 2008, *ApJ*, 675, 1002
- Prochaska, J. X. & Herbert-Fort, S. 2004, *PASP*, 116, 622
- Prochaska, J. X., Herbert-Fort, S., & Wolfe, A. M. 2005, *ApJ*, 635, 123
- Prochaska, J. X. & Wolfe, A. M. 2009, *ApJ*, 696, 1543
- Schaye, J. & Dalla Vecchia, C. 2008, *MNRAS*, 383, 1210
- Springel, V. 2005, *MNRAS*, 364, 1105
- Springel, V. & Hernquist, L. 2003, *MNRAS*, 339, 289
- Tajiri, Y. & Umemura, M. 1998, *ApJ*, 502, 59
- Yajima, H., Choi, J., & Nagamine, K. 2010, *MNRAS*, in press (arXiv:1002.3346)
- Yajima, H., Umemura, M., Mori, M., & Nakamoto, T. 2009, *MNRAS*, 398, 715
- Yang, Y., Zabludoff, A. I., Davé, R., Eisenstein, D. J., Pinto, P. A., Katz, N., Weinberg, D. H., & Barton, E. J. 2006, *ApJ*, 640, 539
- Zheng, Z. & Miralda-Escudé, J. 2002, *ApJ*, 568, L71